small NANO MICRO

Graphene layers

Self-Limited Oxidation: A Route to Form Graphene Layers from Graphite by One-Step Heating

Chunxiao Cong, Ting Yu, Haomin Wang, Kaihong Zheng, Pingqi Gao, Xiaodong Chen, and Qing Zhang*

Graphene, a monolayer of sp^2-bonded carbon atoms, has inspired great enthusiasm since it was successfully isolated from graphite in 2004[1] and especially after the reports of its exceptional relativistic quantum Hall effect in 2005.[2,3] The novel electronic properties involving ballistic transport, massless Dirac fermionlike charge carriers,[2] and Berry's phase[3] in graphene make this two-dimensional material a promising candidate for fundamental studies and nanoelectronics. As such, intensive efforts have been afforded to the formation of graphene layers. Some methods have been developed based on two strategies: top down, such as mechanical exfoliation,[1] evaporating Si atoms from bulk SiC,[4–6] and chemically assisted exfoliation of graphene sheets from bulk graphite;[7–9] and bottom up, such as growth of graphene layers on single or polycrystalline metals.[10–13] Although these methods have their own certain advantages, the extremely fast growth of the demand for graphene layers for various types of fundamental and practical studies strongly urges researchers to develop more novel methods for fabrication of graphene layers.

Herein, we demonstrate a simple yet efficient approach for the formation of graphene layers under the top-down scheme. Our results clearly reveal that graphene layers of good crystal quality could be readily formed by self-limited oxidation of graphite flakes through a one-step annealing process. Because of the feasibility of this method—directly transforming graphite to graphene—many advantages might be adopted, such as simple process, low cost, substrate-friendly or transfer-free fabrication, high yield, good quality, and predetermined locations and patterns of graphene layers. This could be useful for further development of graphene-based nanodevices.

Burning carbon materials is one of the most important and unique activities of human beings. Researchers have been investigating the kinetics of oxidation on carbon, especially graphite, for more than 150 years. The oxidation of graphite could be characterized as three temperature regimes: i) a chemical regime (<500 °C), featuring slow reactions and uniform attack without changing the graphite geometry; ii) a boundary-layer-controlled regime (>900 °C), characterized by fast reactions and nonuniform attack; and iii) an in-pore diffusion-controlled regime, a regime between i and ii, in which gas diffusion in the pore structure of the graphite dominates the reaction rate.[14] A highly anisotropic crystal structure of graphite, which leads to different oxidation rates along different crystallographic lattice directions such as the *a* axis (in-plane or lateral direction) and *c* axis (out-of-plane or vertical direction), together with the unique behavior of boundary-layer-controlled oxidation, might be possible to reduce graphite flakes to graphene layers at elevated temperature as mimetic mechanical exfoliation but with consumption of bulk graphite.

Figure 1a and b show the optical images of graphite flakes after annealing at 900 °C for 60 min with 0.05% oxygen in Ar. From the contrast of optical images, it can be clearly seen that thin graphene sheets were formed at the boundary of graphite flakes. To further identify the number of layers of the as-grown graphene, micro-Raman spectroscopy and mapping were employed, a powerful and unique probe for characterizing graphene.[15–19] The Raman spectrum of perfect graphene is dominated by two strong and sharp peaks, namely the G band, a zero-momentum phonon–electron scattering, and the 2D (or G') band, a two-phonon (2iTO)–electron double resonance scattering. The difference in electronic spectra of mono- (MLG) and double-layer graphene (DLG) results in the varieties of 2D band of Raman spectra. For example, extra branches near the K-point at low energy level of DLG cause additional subpeaks in the 2D band and increment of the line width.[20] Another band, the D band resulting from defect-assisted double resonance scattering, could be observed in graphene with the existence

Dr. C. X. Cong, Prof. T. Yu, Dr. H. M. Wang
Division of Physics and Applied Physics
School of Physical and Mathematical Sciences
Nanyang Technological University
Singapore 637371, Singapore
E-mail: yuting@ntu.edu.sg
Prof. T. Yu
Department of Physics
Faculty of Science
National University of Singapore
117542, Singapore
Dr. K. H. Zheng, Prof. X. D. Chen
Materials Science and Engineering
Nanyang Technological University
50 Nanyang Avenue, Singapore 639798, Singapore
Dr. P. Q. Gao, Prof. Q. Zhang
Microelectronics Center
School of Electrical and Electronic Engineering
Nanyang Technological University
S1-B2c-20, Singapore 639798, Singapore

DOI: 10.1002/smll.201001184

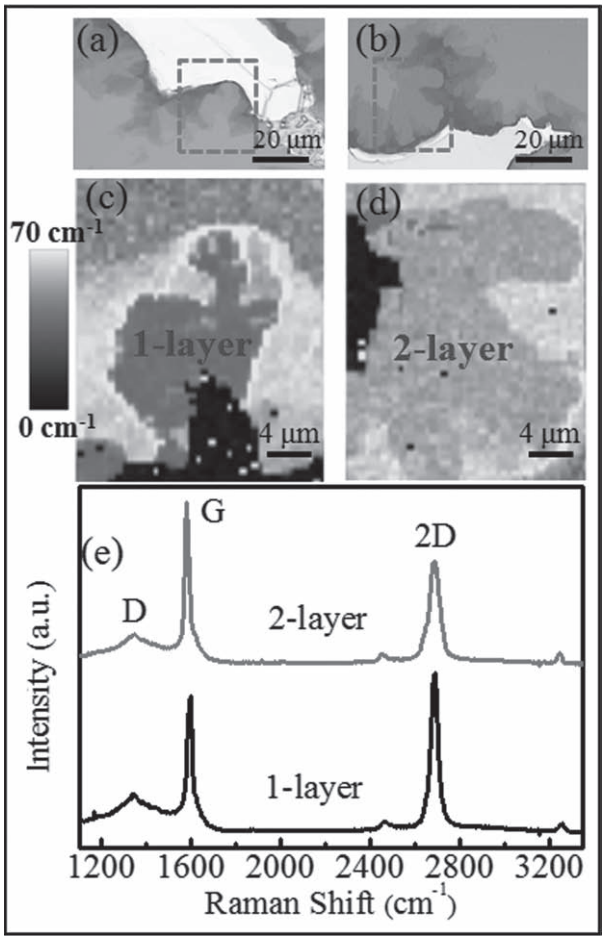

Figure 1. a,b) Optical images of graphene layers formed by self-limited oxidation of graphite. c,d) 2D line-width Raman images of the graphene layers highlighted in (a) and (b). e) Raman spectra of the as-grown mono- and double-layer graphene flakes.

of defects, and the integrated intensity ratio between G and D bands is a widely accepted indicator of the crystal quality of graphene.[19] Figure 1c and d present the 2D line-width Raman images of the areas of interest highlighted in Figure 1a and b, unambiguously revealing the formation of MLG and DLG tens of micrometers in dimension. The weak D bands (Figure 1e) indicate the good crystal quality of the as-grown graphene layers.

Previous studies on the oxidation of graphite revealed that oxidation starts at defects, such as a carbon vacancy, mechanical deformation, adsorbed impurity, and edges.[21–23] To demonstrate the effects of defects on the oxidation, graphite flakes from highly oriented pyrolytic graphite (HOPG) were treated under the same conditions (900 °C, 0.05% oxygen in Ar with a flow rate of 50 sccm). As shown in Figure S1 in the Supporting Information, both the boundary and some parts in the body of pristine graphite flakes where defects locate are severely etched. Thin layers of graphene could be observed at the boundaries of the graphite plate and the etched pits. Here, we are more interested in graphite flakes from natural crystals, in which the majority of defects are edges. Thus, the oxidation starts with attack on carbon atoms at the edges owing to the fact that these carbon atoms exhibit a greater reactivity than those within the layer planes because of the higher electron density caused by the dangling bonds.[21,24] **Figure 2**a and b are optical images of a partially folded graphite plate before and after annealing at 900 °C. The critical role of carbon atoms possessing dangling bonds on the oxidation can be clearly seen by the much more significant etch of the nonfolded edge compared to that of the folded edge. The as-grown graphene layers were also characterized by scanning electron microscopy (SEM; Figure 2c). From both optical (Figure 2c, inset) and SEM images, a thin-layer region is located. The depth profile of this region was explored by atomic force microscopy (AFM; Figure 2d), which indicates that the oxidation happens to the top layer first, then the layer below. Alternatively, the layer(s) just on top of the substrate remained. It is noted that the dimension of the remaining thick graphite plate shows a more significant decrease than that of the piece including both graphite plate and graphene layers. In other words, the lateral etch rate is faster in the top layers of graphite than that in the few layers at the very bottom. The oxidation rate of these few layers is limited and eventually this limitation leads to the formation of graphene layers. The self-limited phenomena are quite interesting, and the reduction mechanism behind them should be different from that of reduction layer by layer.[25] This self-limited oxidation, which removes carbon atoms from the

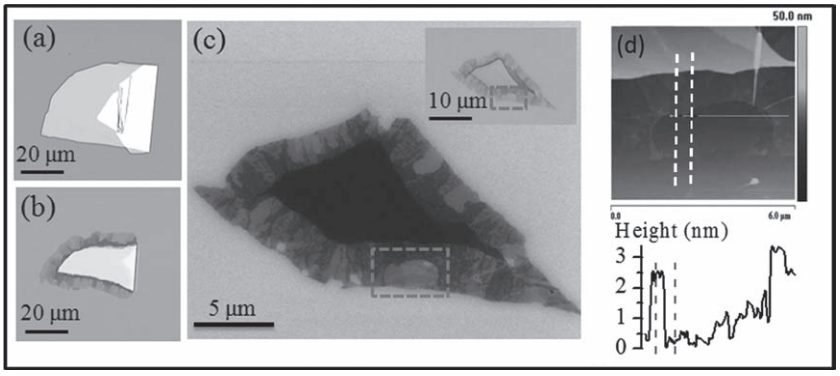

Figure 2. a,b) Optical images of partially folded graphite flakes before and after the self-limited oxidation process. c) SEM image of a graphite plate after oxidation. Inset: the corresponding optical image. d) AFM image and height profile of the graphene layers highlighted in (c).

small NANO MICRO

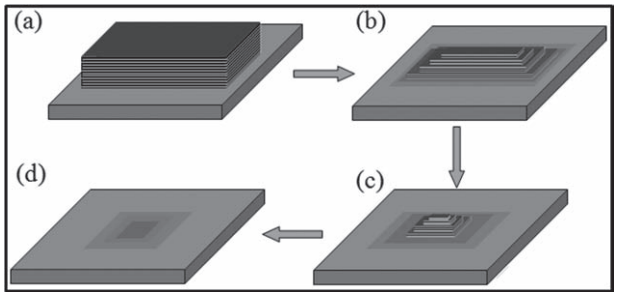

Figure 3. Schematic diagram of the formation of graphene layers from graphite flakes by a self-limited oxidation process.

edges of layer planes, is also different from that of graphene oxidation, in which an etching reaction occurs in basal planes of graphene sheets.[26]

To further understand the growth mechanism, the temperature dependence of the formation of graphene layers was exploited by heating the graphite flakes at different temperatures; the corresponding optical images are shown in Figure S2 in the Supporting Information. For the sample annealed at a relatively low temperature (800 °C), the whole plate becomes slightly smaller without forming graphene layers. When the heating temperature reaches 900 °C and beyond, graphene layers are formed and a higher temperature leads to bigger pieces or a more significant oxidation-limited effect. Based on the discussion above, at 900 °C and above the oxidation mainly starts at the boundary, and the lateral oxidation rate is significantly faster than the vertical rate; thus, we propose a self-limited oxidation process to explain the formation of graphene layers in this work. As illustrated by the schematic diagrams in **Figure 3**, oxygen molecules attack carbon atoms at the edge of the top layers first. Due to the significantly faster lateral oxidation rate relative to the vertical rate, the original edge part of the top layers is removed quickly and the layers below are uncovered, therefore being exposed to oxygen and following the same reaction as in the top layers. So, at the initial heating stage, multilayer-edge steps are formed (Figure 3b). Depending on the thickness of the pristine graphite flakes, such multilayer edges might be composed of several hundreds to thousands of layers. Our results show that graphene layers could be formed from graphite flakes in a quite wide range of thicknesses. Once a few layers at the bottom or eventually the layer just on top of the substrate is uncovered, the lateral oxidation rates of these few layers and monolayer are slowed down dramatically while the lateral oxidation rate of multilayer-edge steps remains. This is because the oxidation rate coefficient, a measure of the ease of oxidation of carbon atoms exposed, of multilayer-edge steps is nearly a hundred times the corresponding rate of the monolayer edge and around ten times that of few-layer edges, a result of a cooperative effect.[26,27] Thus, the oxidation of the few layers and monolayer along the lateral direction is self-limited by the nature of the oxidation of graphite. Hence, at the middle stage of heating, the few-layer graphene (FLG) and MLG are uncovered (Figure 3c), and the dimension as well as the relative portion of FLG and MLG relative to the remaining graphite increase with heating duration although they are also being etched slowly. Finally, the MLG together with some BLG and FLG sheets are formed (Figure 3d). Further optimizing the growth conditions could form pure single-layer graphene sheets.

In the present work, the influence of oxygen concentration and flow rate on the formation of graphene layers was also investigated. From the optical images (Figure S3, Supporting Information), the low oxygen concentration of 0.05% is critical to form graphene layers. Too much oxygen could burn the whole graphite flake (Figure S3a) or break the self-limited oxidation by leaving no graphene layers (Figure S3b). For the gas flow rate, our results (Figure S4, Supporting Information) indicate that graphene layers could be formed within a wide range, that is, 50–400 sccm. A higher flow rate than 400 sccm may introduce more severe turbulence and result in a very rough boundary.

Graphene layers could now be fabricated by directly transforming graphite flakes. This promises feasibility in the controllable formation of graphene layers, such as shape, location, and pattern control through controlling the corresponding features of mother graphite flakes. **Figure 4** presents an example of such control. Parallel graphene ribbons are readily formed by converting entire prepatterned graphite belts. The 2D line-width Raman mapping indicates that the graphene ribbons are dominated by MLG and DLG, but with some small fraction of MLG. With further optimization of the parameters, pure MLG nanoribbons or nanotriangles might be able to be fabricated, which could be very important for the fundamental studies and practical applications of

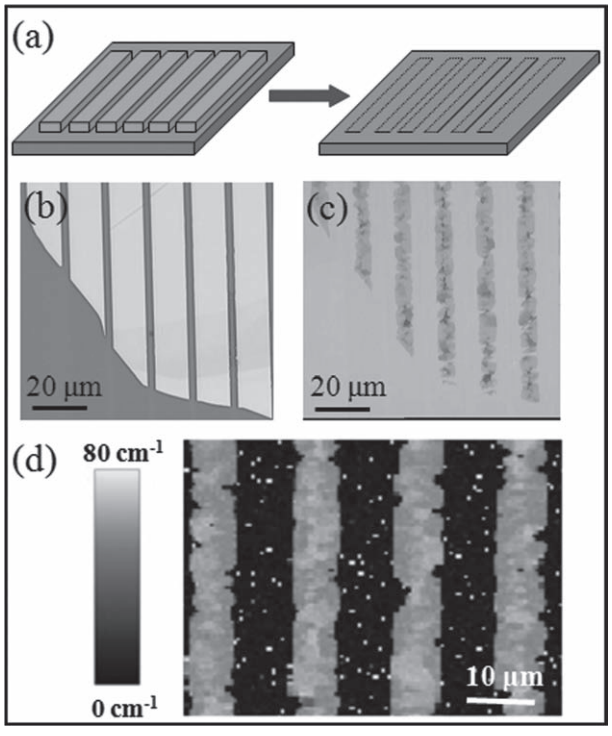

Figure 4. a) Schematic diagram of patterned graphene layers formed from prepatterned graphite by a self-limited oxidation procedure. b,c) Optical images of prepatterned graphite and graphene ribbons, respectively. d) Raman image of the patterned graphene ribbons obtained by extracting the width of the 2D mode.

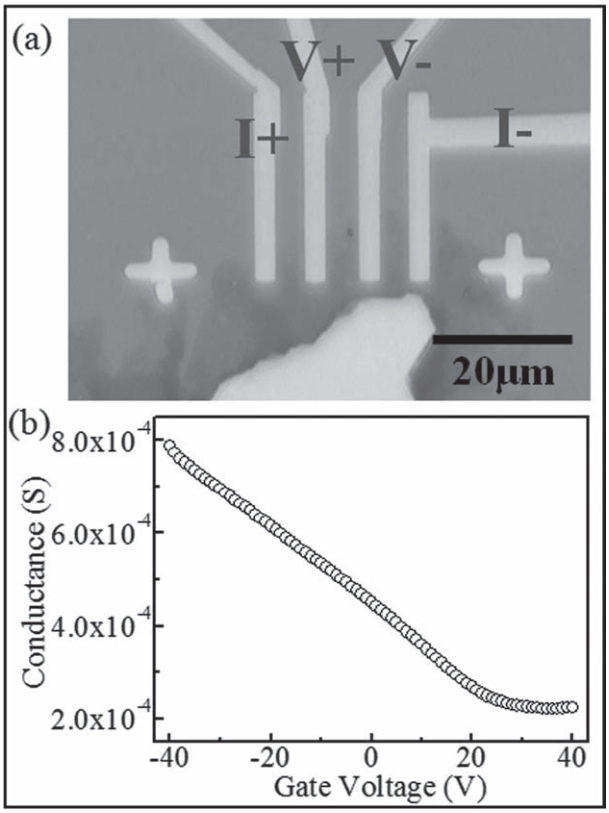

Figure 5. a) Optical image of a graphene field-effect transistor with a four-probe configuration. b) Conductance as a function of back-gate voltage.

graphene in nanoelectronics and nanospintronics. Substrate-friendly or transfer-free fabrication is another unique advantage of this technique. Graphene layers have been fabricated by directly heating graphite flakes on various types of substrates, such as Si, SiC, and GaN. Figure S5 in the Supporting Information shows the SEM image and Raman spectrum of DLG formed on a Si substrate.

To demonstrate the quality of the as-grown graphene layers, electrical transport measurements were conducted. **Figure 5**a shows the optical image of a DLG (predetermined by Raman spectroscopy) device in four-probe configuration. The graphene sheet was produced by the self-limited oxidation procedure. The conductance as a function of back-gate voltage (V_g) is shown in Figure 5b. It can be seen that the graphene sheet was p-doped with the neutral point at around 35 V. The hole mobility $\mu = (1/C_g)\,|d\sigma/dV_g|$ is estimated to be about 500 $cm^2\ V^{-1}\ s^{-1}$, where σ is the conductivity and $C_g = \varepsilon\varepsilon_0/d$ (ε is the dielectric constant of SiO_2, ε_0 is the permittivity of free space, and $d = 300$ nm).

In summary, graphene layers of good crystal quality have been readily formed by one-step heating of graphite flakes with a self-limited oxidation mechanism. The unique advantages associated with this technique, such as simple process, low cost, substrate-friendly or transfer-free fabrication, and location, shape, and pattern control, indicate its promising potential in the controllable formation of graphene layers and graphene nanostructures for future fundamental studies and practical applications.

Experimental Section

Large numbers of graphite flakes were obtained by mechanical exfoliation of single-crystal graphite on silicon substrates covered with 300 nm of thermal silicon oxide. The graphite samples were introduced to a quartz tube furnace and subjected to heating processes at different temperatures (800–1000 °C) in a flow of O_2 in Ar of various concentrations (5, 0.5, and 0.05%) and flow rates (50–400 sccm). Tens of micrometers graphene layers were formed at the boundary of graphite flakes. The graphene layers were characterized by optical microscopy, AFM (Veeco Dimension V), low-voltage SEM (JOEL JSM-6700F), and Raman mapping/spectroscopy (WITEC CRM200 confocal system, $\lambda_{laser} = 532$ nm). To avoid a heating effect, the laser power at the sample surface was fixed at 0.5 mW. Au/Cr (30/5 nm) electrodes were formed on selected graphene layers by using a combination of electron-beam lithography and evaporation-based lift-off processes. The electrical measurements were performed using a four-probe configuration under ambient conditions.

Supporting Information

Supporting Information is available from the Wiley Online Library or from the author.

Acknowledgements

This work was supported by the Singapore National Research Foundation under NRF RF Award No. NRF-RF2010–07 and MOE Tier 2 MOE2009-T2–1-037.

[1] K. S. Novoselov, A. K. Geim, S. V. Morozov, D. Jiang, Y. Zhang, S. V. Dubonos, I. V. Grigorieva, A. A. Firsov, *Science* **2004**, *306*, 666.
[2] K. S. Novoselov, A. K. Geim, S. V. Morozov, D. Jiang, M. I. Katsnelson, I. V. Grigorieva, S. V. Dubonos, A. A. Firsov, *Nature* **2005**, *438*, 197.
[3] Y. Zhang, Y. W. Tan, H. L. Stormer, P. Kim, *Nature* **2005**, *438*, 201.
[4] C. Berger, Z. M. Song, X. B. Li, X. S. Wu, N. Brown, C. Naud, D. Mayou, T. B. Li, J. Hass, A. N. Marchenkov, E. H. Conrad, P. N. First, W. A. de Heer, *Science* **2006**, *312*, 1191.
[5] T. Ohta, A. Bostwick, T. Seyller, K. Horn, E. Rotenberg, *Science* **2006**, *313*, 951.
[6] I. Forbeaux, J. M. Themlin, J. M. Debever, *Phys. Rev. B* **1998**, *58*, 16396.
[7] Y. Hernandez, V. Nicolosi, M. Lotya, F. M. Blighe, Z. Sun, S. De, I. T. McGovern, B. Holland, M. Byrne, Y. K. Gun'ko, J. J. Boland, P. Niraj, G. Duesberg, S. Krishnamurthy, R. Goodhue, J. Hutchison, V. Scardaci, A. C. Ferrari, J. N. Coleman, *Nat. Nanotechnol.* **2008**, *3*, 563.
[8] P. Blake, P. D. Brimicombe, R. R. Nair, T. J. Booth, D. Jiang, F. Schedin, L. A. Ponomarenko, S. V. Morozov, H. F. Gleeson, E. W. Hill, A. K. Geim, K. S. Novoselov, *Nano Lett.* **2008**, *8*, 1704.
[9] M. Lotya, Y. Hernandez, P. J. King, R. J. Smith, V. Nicolosi, L. S. Karlsson, F. M. Blighe, S. De, Z. Wang, I. T. McGovern, G. S. Duesberg, J. N. Coleman, *J. Am. Chem. Soc.* **2009**, *131*, 3611.

[10] P. W. Sutter, J.-I. Flege, E. A. Sutter, *Nat. Mater.* **2008**, *7*, 406.
[11] R. van Gastel, A. T. N'Diaye, D. Wall, J. Coraux, C. Busse, N. M. Buckanie, F.-J. Meyer zu Heringdorf, M. Horn von Hoegen, T. Michely, B. Poelsema, *Appl. Phys. Lett.* **2009**, *95*, 121901.
[12] Y. Gamo, A. Nagashima, M. Wakabayashi, M. Terai, C. Oshima, *Surf. Sci.* **1997**, *374*, 61.
[13] K. S. Kim, Y. Zhao, H. Jang, S. Y. Lee, J. M. Kim, K. S. Kim, J.-H. Ahn, P. Kim, J.-Y. Choi, B. H. Hong, *Nature* **2009**, *457*, 706.
[14] L. Snead, T. Burchell, Oxidation of High-Quality Graphite for IFE, http://www-ferp.ucsd.edu/HAPL/MEETINGS/0111-HAPL/snead_g_oxidation.doc (last accessed October, 2010).
[15] Z. H. Ni, H. M. Wang, J. Kasim, H. M. Fan, T. Yu, Y. H. Wu, Y. P. Feng, Z. X. Shen, *Nano Lett.* **2007**, *7*, 2758.
[16] T. Yu, Z. Ni, C. Du, Y. You, Y. Wang, Z. Shen, *J. Phys. Chem. C* **2008**, *112*, 12602.
[17] Z. Luo, T. Yu, K. Kim, Z. Ni, Y. You, S. Lim, Z. Shen, S. Wang, J. Lin, *ACS Nano* **2009**, *3*, 1781.
[18] L. M. Malard, M. A. Pimenta, G. Dresselhaus, M. S. Dresselhaus, *Phys. Rep.* **2009**, *473*, 51.
[19] A. C. Ferrari, *Solid State Commun.* **2007**, *143*, 45.
[20] A. C. Ferrari, J. C. Meyer, V. Scardaci, C. Casiraghi, M. Lazzeri, F. Mauri, S. Piscanec, D. Jiang, K. S. Novoselov, S. Roth, A. K. Geim, *Phys. Rev. Lett.* **2006**, *97*, 187401.
[21] J. R. Hahn, *Carbon* **2005**, *43*, 1506.
[22] A. Tracz, G. Wegner, J. P. Rabe, *Langmuir* **1993**, *9*, 3033.
[23] W. R. Smith, M. H. Polly, *J. Phys. Chem.* **1956**, *60*, 689.
[24] K. H. Lee, H. M. Lee, H. M. Eun, W. R. Lee, S. Kim, D. Kim, *Surf. Sci.* **1994**, *312*, 217.
[25] H. M. Wang, Y. H. Wu, Z. H. Ni, Z. X. Shen, *Appl. Phys. Lett.* **2008**, *92*, 053504.
[26] L. Liu, S. Ryu, M. R. Tomasik, E. Stolyarova, N. Jung, M. S. Hybertsen, M. L. Steigerwald, L. E. Brus, G. W. Flynn, *Nano Lett.* **2008**, *8*, 1965.
[27] E. L. Evans, R. J. M. Griffiths, J. M. Thomas, *Science* **1971**, *171*, 174.
[28] C. Wong, R. T. Yang, *Carbon* **1982**, *20*, 253.

Received: July 13, 2010
Revised: September 1, 2010
Published online: November 10, 2010

